

AD-751 573

SIGNAL-TO-NOISE RATIOS REQUIRED FOR SHORT-
TERM NARROWBAND DETECTION OF GAUSSIAN
PROCESSES

Albert H. Nuttall, et al

Naval Underwater Systems Center
Newport, Rhode Island

20 October 1972

DISTRIBUTED BY:

NTIS

National Technical Information Service
U. S. DEPARTMENT OF COMMERCE
5285 Port Royal Road, Springfield Va. 22151

NUSC Technical Report 4417

AD751573

Signal-to-Noise Ratios Required for Short-Term Narrowband Detection of Gaussian Processes

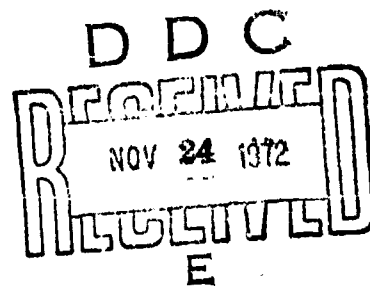
ALBERT H. NUTTALL

Office of the Director of Science and Technology

ANTHONY F. MAGARACI

Submarine Sonar Department

20 October 1972

**NAVAL UNDERWATER SYSTEMS CENTER**

Reproduced by
NATIONAL TECHNICAL
INFORMATION SERVICE
U S Department of Commerce
Springfield VA 22151

Approved for public release; distribution unlimited.


32
R

ADMINISTRATIVE INFORMATION

This report was prepared for Principal Investigator, G. F. Carey (Code SA1). The sponsoring activity is the Naval Ship Systems Command, Project Manager, CDR R. B. Gilchrist, (Code PMS-302-5). It was also prepared under NUSC Project No. A-752-05, "Statistical Communication with Applications to Sonar Signal Processing" (U), Principal Investigator, Dr. A. H. Nuttall (Code TC); and Subproject and Task No. ZF XX 212 001. The sponsoring activity is Chief of Naval Material, Program Manager, Dr. J. H. Huth.

The Technical Reviewer for this report was H. S. Newman (Code TD111).

REVIEWED AND APPROVED: 20 October 1972


W. A. Von Winkle
Director of Science and Technology

A

Inquiries concerning this report may be addressed to the authors,
New London Laboratory, Naval Underwater Systems Center,
New London, Connecticut 06320

UNCLASSIFIED

Security Classification

DOCUMENT CONTROL DATA - R & D*(Security classification of title, body of abstract and indexing annotation must be entered when the overall report is classified)*

1. ORIGINATING ACTIVITY (Corporate author) Naval Underwater Systems Center Newport, Rhode Island 02840		2a. REPORT SECURITY CLASSIFICATION UNCLASSIFIED	
		2b. GROUP	
3. REPORT TITLE SIGNAL-TO-NOISE RATIOS REQUIRED FOR SHORT-TERM NARROWBAND DETECTION OF GAUSSIAN PROCESSES			
4. DESCRIPTIVE NOTES (Type of report and inclusive dates) Research Report			
5. AUTHOR(S) (First name, middle initial, last name) Albert H. Nuttall Anthony F. Magaraci			
6. REPORT DATE 20 October 1972		7a. TOTAL NO. OF PAGES 36	7b. NO. OF REFS 10
8a. CONTRACT OR GRANT NO.		9a. ORIGINATOR'S REPORT NUMBER(S) TR 4417	
b. PROJECT NO A-752-05 ZF XX 212 001			
c.		9b. OTHER REPORT NO(S) (Any other numbers that may be assigned this report)	
d.			
10. DISTRIBUTION STATEMENT Approved for public release; distribution unlimited.			
11. SUPPLEMENTARY NOTES		12. SPONSORING MILITARY ACTIVITY Department of the Navy	
13. ABSTRACT <p>The required signal-to-noise ratios for short-term detection of a narrowband Gaussian signal process in Gaussian noise are computed for false alarm probabilities 10^{-n}, $n = 1(1)8$; detection probabilities 0.5, 0.7, 0.9, 0.99; and observation-time analysis-bandwidth products in the range of 0 to 100. No assumptions are made about Gaussian statistics of the decision variable, or about long observation intervals. It is found that the required signal-to-noise ratios are significantly greater in some cases than those predicted from a simple deflection criterion of system performance.</p>			

UNCLASSIFIED

Security Classification

14. KEY WORDS	LINK A		LINK B		LINK C	
	ROLE	WT	ROLE	WT	ROLE	WT
Narrowband Detection						
Short-Term Detection						
Required Signal-to-Noise Ratio						
Gaussian Processes						
False Alarm Probability						
Detection Probability						
Equivalent Number of Independent Samples						

TABLE OF CONTENTS

	Page
ABSTRACT	i
LIST OF ILLUSTRATIONS	v
LIST OF TABLES	v
LIST OF ABBREVIATIONS AND SYMBOLS	vii
INTRODUCTION	1
PROBLEM DEFINITION	2
PROBLEM SOLUTION	3
RESULTS	5
CONCLUSIONS AND RECOMMENDATIONS	13
APPENDIX A — EQUIVALENT NUMBER OF INDEPENDENT SQUARED-ENVELOPE SAMPLES	15
APPENDIX B — THRESHOLD VALUES	23
APPENDIX C — GAUSSIAN APPROXIMATION	25
LIST OF REFERENCES	27

LIST OF ILLUSTRATIONS

Figure		Page
1	Narrowband Detector	2
2	Required Signal-to-Noise Ratio for $P_D = .5$	6
3	Required Signal-to-Noise Ratio for $P_D = .7$	7
4	Required Signal-to-Noise Ratio for $P_D = .9$	8
5	Required Signal-to-Noise Ratio for $P_D = .99$	9
6	Comparison of Exact Results, Gaussian Approximation, and Sine-Wave Signal	11
A-1	Equivalent Number of Independent Squared-Envelope Samples for Rectangular Spectrum	19
A-2	Equivalent Number of Independent Squared-Envelope Samples for Gaussian Spectrum	20
A-3	Equivalent Number of Independent Squared-Envelope Samples for Cauchy Spectrum	22

LIST OF TABLES

Table		Page
1	Additive Constant in (12)	10
B-1	Normalized Threshold Values A	23

LIST OF ABBREVIATIONS AND SYMBOLS

SNR	Signal-to-noise ratio
NBF	Narrowband filter
SE	Squared-envelope
RV	Random variable
t	Time
$x(t)$	Input waveform
$s(t)$	Input signal
$n(t)$	Input noise
B	Signal and narrowband filter bandwidth
T	Observation (averaging) time
$\varepsilon(t)$	Envelope
$\varepsilon^2(t)$	Squared-Envelope
Λ	Threshold
z	Decision variable
σ^2	Narrowband filter output power
N	Noise power at NBF output
S	Signal power at NBF output
f	Frequency
$G_y(f)$	Spectrum of process $y(t)$
M	Number of independent samples
w_k	Envelope samples
p	Probability density function
Prob()	Probability of ()
P_F	Probability of false alarm
P_D	Probability of detection
A	Normalized threshold
Φ	Cumulative Gaussian distribution (equation (C-5))
Φ^{-1}	Inverse Φ -function

SIGNAL-TO-NOISE RATIOS REQUIRED FOR SHORT-TERM NARROWBAND DETECTION OF GAUSSIAN PROCESSES

INTRODUCTION

Rules of thumb are available for approximating the required signal-to-noise ratio (SNR) for broadband and narrowband energy detection of signals in noise (see reference 1). However, they are generally applicable or appropriate only when certain requirements (long observation (averaging) time, for example) are satisfied. Attempts to apply these rules outside their often ill-defined ranges of applicability can result in very misleading conclusions about system performance and capability. This is particularly true for high-resolution, narrowband detection systems where the analysis bandwidth is so small that practical observation times lead to only a few effectively independent samples of the processes under investigation; this is called short-term detection here.

The rules of thumb may be inapplicable because they are often based on a deflection criterion of system performance, such as the square of the difference of the mean outputs, with and without signal, divided by some variance of the system output. Since these rules use only first and second moments of the system output decision variable, they are incomplete statistical descriptors. Furthermore, the two lowest moments are often employed in a Gaussian approximation in order to estimate probabilities of detection and false alarms. This approach can lead to an obvious contradiction, such as stating that no value of SNR, no matter how large, will yield very high detection probabilities for a limited observation time. *

The best way to avoid such situations, and the approach this report discusses, is to evaluate the exact probability distribution of the decision variable without making a Gaussian assumption — a method that is particularly relevant in short-term detection where only a few independent samples of the system output are available.

*See, for example, reference 1, equations (37) through (40), where deflection criteria P_1 and P_2 can not exceed TW_s , and, in fact, the required $S_0/N_0 \rightarrow \infty$ as $P_1, P_2 \rightarrow TW_s$.

PROBLEM DEFINITION

The detector of interest here is depicted in figure 1. The input $x(t)$ is composed of stationary, zero-mean, Gaussian signal $s(t)$ and noise $n(t)$, or noise $n(t)$ alone. It is assumed that the narrowband filter (NBF) is centered on the signal and has the same bandwidth, B Hz, as the signal spectrum. (The effects of over-resolution and under-resolution, and of mismatched center frequencies, are discussed in reference 1.) The input noise is assumed to be fairly flat over a frequency interval wider than B Hz. The sampler takes a sample of the squared-envelope (SE) $\varepsilon^2(t)$ approximately every B^{-1} sec, * accumulating these SE samples for an observation interval of T sec. The threshold, Λ , with which z is compared, is fixed. (The effects of using a tracking threshold based on a few noise-alone frequency bins are discussed in reference 1 and thoroughly investigated in reference 2.)

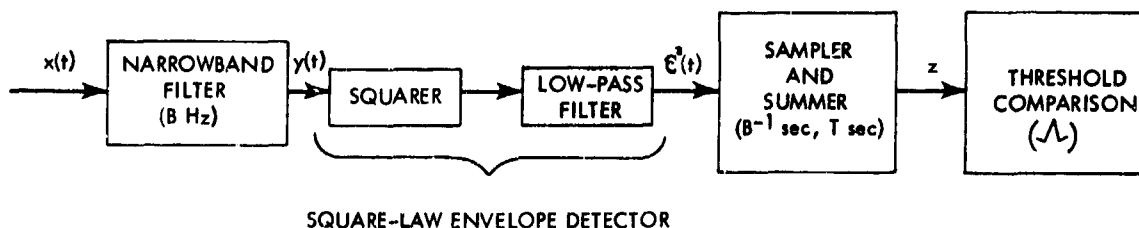


Figure 1. Narrowband Detector

If, after an observation interval of T sec, random variable (RV) z exceeds Λ when a signal is absent, a false alarm occurs. It should be noted that this false alarm definition applies to just one NBF, not to a bank of NBFs. Also, a false alarm can occur only once every T sec, not every B^{-1} sec. If Λ is exceeded with a signal present, a detection occurs. The problem, then, is to calculate the false alarm and detection probabilities of the detector in figure 1 as a function of the input SNR.

*This is a reasonable rule for analysis filters with fairly rectangular pass-band characteristics, but samples should be taken more often for filters with rounded characteristics. In the latter case, however, the SE samples are statistically dependent. (Appendix A provides a method for dealing with this dependency.)

PROBLEM SOLUTION

The process $y(t)$ at the NBF output has power σ^2 , where

$$\sigma^2 = \begin{cases} N, & \text{noise-alone input to NBF} \\ S + N, & \text{signal-plus-noise input to NBF} \end{cases} . \quad (1)$$

That is, N is the noise power at the NBF output, and S (if present) is the signal power at the NBF output. These are the powers in the B Hz bandwidth and are not spectral levels in a 1-Hz band.

It will be assumed that the samples every B^{-1} sec at the NBF (or detector) output are statistically independent. This is a fair approximation* if B is interpreted as the effective bandwidth of the signal process and the NBF; that is,

$$B \equiv \frac{\left[\int_0^\infty df G_y(f) \right]^2}{\int_0^\infty df G_y^2(f)} , \quad (2)$$

where $G_y(f)$ is the NBF output power density spectrum. The number of independent SE samples in observation interval T sec is, then, $BT + 1$ and will be denoted by M . (The equivalent number of independent SE samples in interval T for statistically dependent SE samples is considered in Appendix A.)

The generic problem, therefore, is that of calculating the cumulative distribution of the RV z ,

$$z = \sum_{k=1}^M w_k^2 , \quad (3)$$

*See footnote on p. 2.

where w_k are statistically independent samples of the envelope of a narrow-band Gaussian process. Random variable z is a multiple of a chi-square variate with $2M$ degrees of freedom. The probability density function of envelope w_k (reference 3, equations (3.7-5) and (3.7-10)) is given by

$$p(w_k) = \frac{w_k}{\sigma^2} \exp\left(-\frac{w_k^2}{2\sigma^2}\right), \quad w_k > 0 \quad (4)$$

Therefore the probability density function of z (reference 4, equations (2.1), (2.3), and (2.13)) is

$$p(z) = \frac{1}{(M-1)! 2\sigma^2} \left(\frac{z}{2\sigma^2}\right)^{M-1} \exp\left(-\frac{z}{2\sigma^2}\right), \quad z > 0 \quad (5)$$

The probability that RV z exceeds Λ is

$$\begin{aligned} \text{Prob}(z > \Lambda) &= \int_{\Lambda}^{\infty} dz p(z) \\ &= \int_{\Lambda}^{\infty} dt \frac{t^{M-1} e^{-t}}{(M-1)!} = \exp\left(-\frac{\Lambda}{2\sigma^2}\right) \sum_{m=0}^{M-1} \frac{1}{m!} \left(\frac{\Lambda}{2\sigma^2}\right)^m, \end{aligned} \quad (6)$$

the last step via repeated integration by parts.

The probability of false alarm, P_F , and the probability of detection, P_D , are obtained by using (1) in (6):

$$P_F = \exp(-A) \sum_{m=0}^{M-1} \frac{1}{m!} A^m, \quad (7)$$

$$P_D = \exp\left(-\frac{A}{1+S/N}\right) \sum_{m=0}^{M-1} \frac{1}{m!} \left(\frac{A}{1+S/N}\right)^m, \quad (8)$$

where we have defined normalized threshold, A , as

$$A = \frac{\Lambda}{2N} \quad (9)$$

Again, S/N is the ratio of signal power to noise power at the NBF output in figure 1 in the B Hz bandwidth; it is not the spectral level in a 1-Hz band.

Equation (7) can be solved for normalized threshold A for a specified P_F and number of independent SE samples M . (A table for $M = 1(1)10, 16, 32$, and 64 , and $P_F = 10^{-n}$, $n = 1(1)8$, is presented in Appendix B.) Then, for a specified P_D , (8) can be solved for the required values of S/N .

RESULTS

Curves of required S/N in decibels are presented in figures 2 through 5 for $P_D = .5, .7, .9$, and $.99$, respectively. Values of P_F equal to 10^{-n} , $n = 1(1)8$, are considered for a range of M from 1 to 100. (Since the curves were evaluated only at the integer points, straight-line interpolation was used for ease of reading.) M is to be interpreted as $BT + 1$ in figure 1 and is the equivalent number of independent SE samples in observation time T .

It will be observed from figures 2 through 5 that the required S/N increases rapidly as M decreases. In fact, the required value of S/N for $M = 1$ is given by

$$S/N = \frac{\ln P_F}{\ln P_D} - 1, (M = 1); \quad (10)$$

this result follows from (7) and (8). Thus for values of P_D near unity, a very large value of S/N is required for $M = 1$.

On the other hand, the curves are fairly similar for large M , there being, for example, 1.9 dB more SNR required (at $M = 100$, $P_F = 10^{-3}$) for $P_D = .9$ than for $P_D = .5$.

The difference between the curves decreases as P_D is increased in figures 2 through 5. Part of this difference is the result of the change of the ordinate scale in each figure, but part of it is a real effect. For example, the difference between the curves at $M = 100$, $P_D = .5$ is 2.1 dB, whereas the difference between the curves at $M = 100$, $P_D = .99$ is 1.4 dB. The corresponding differences at $M = 1$ are 3.25 and 3.0 dB, respectively.

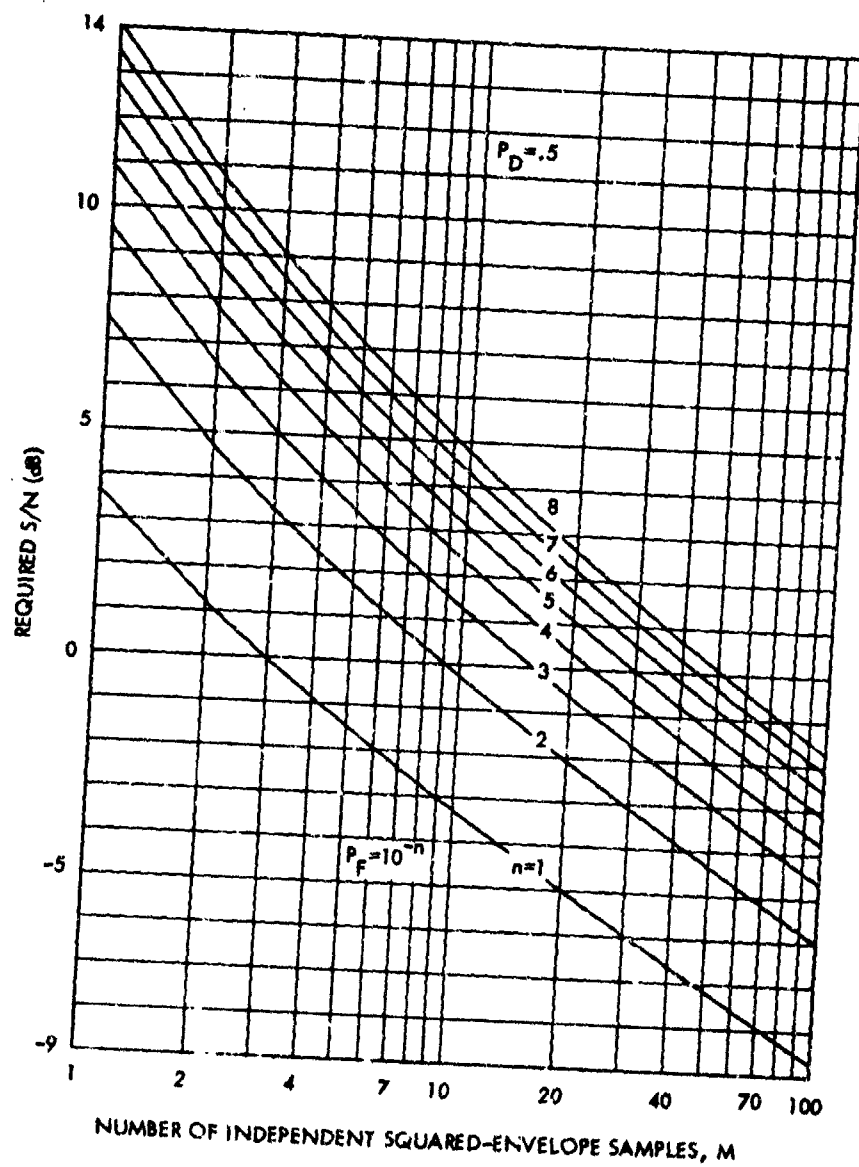


Figure 2. Required Signal-to-Noise Ratio for $P_D = 0.5$

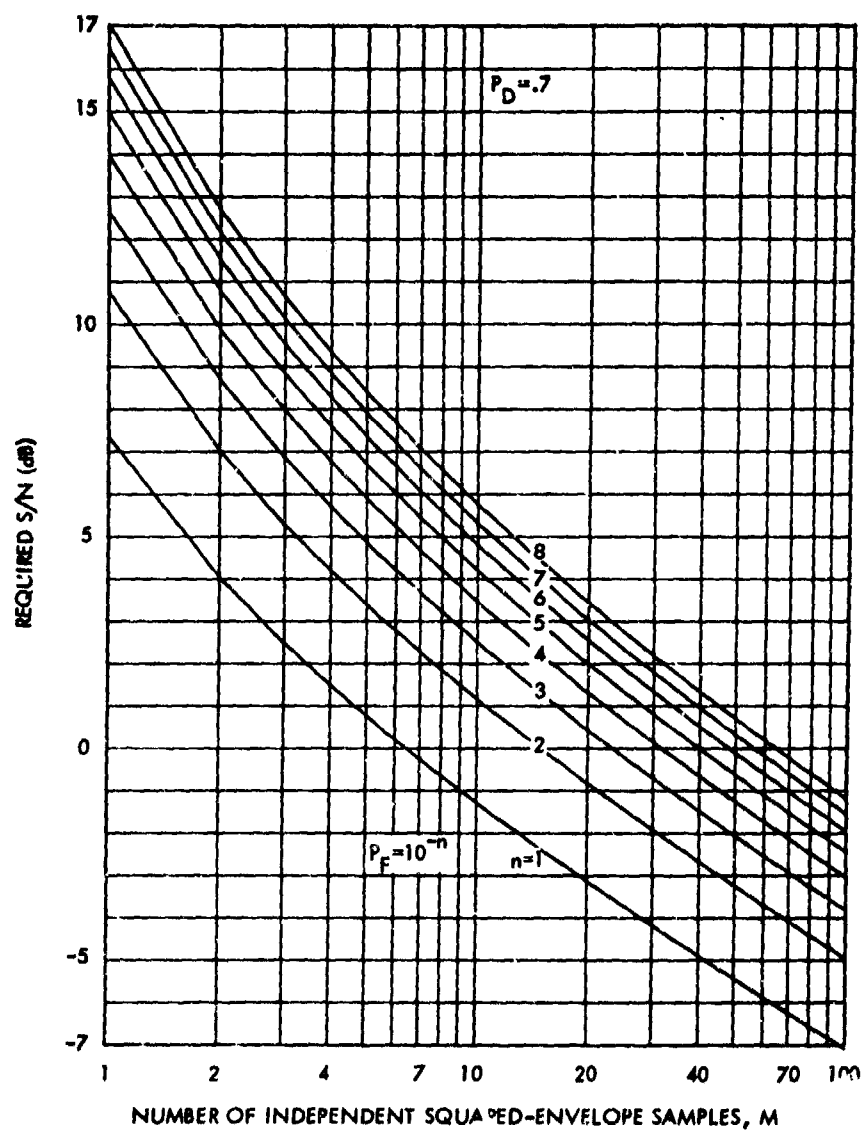


Figure 3. Required Signal-to-Noise Ratio for $P_D = .7$

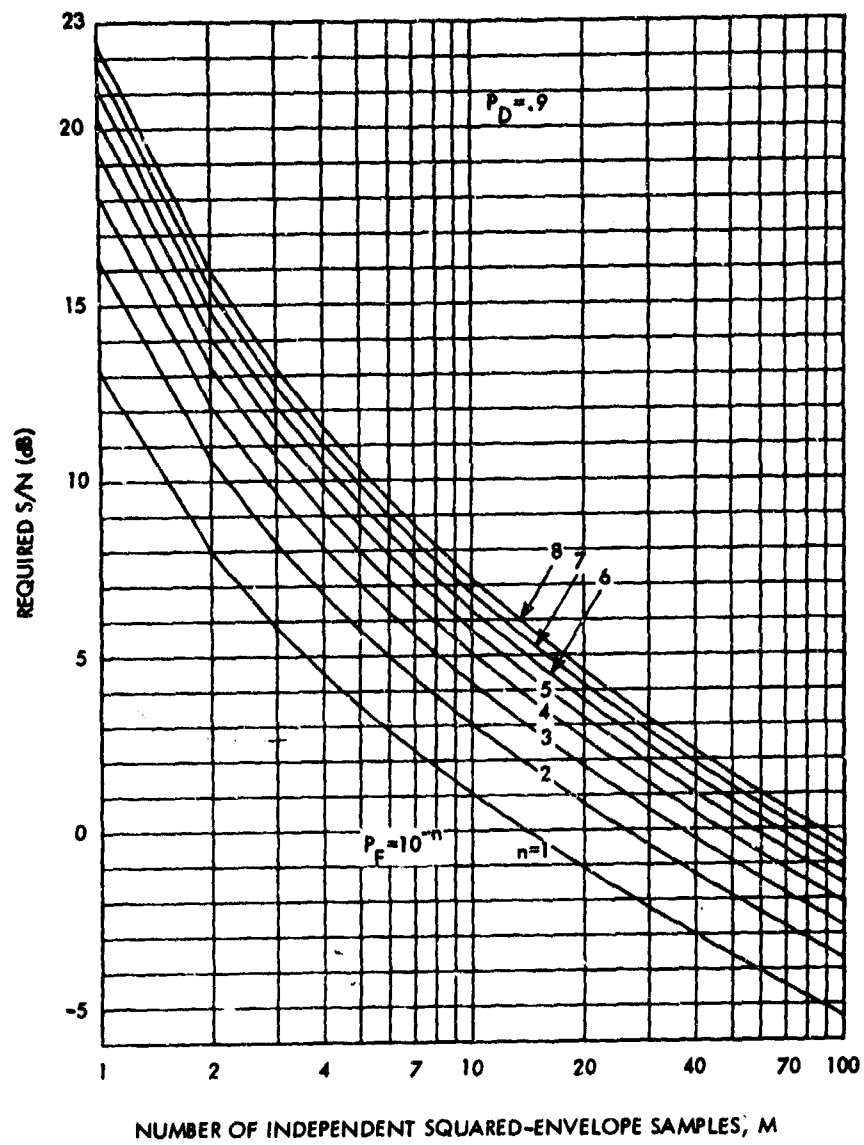


Figure 4. Required Signal-to-Noise Ratio for $P_D = .9$

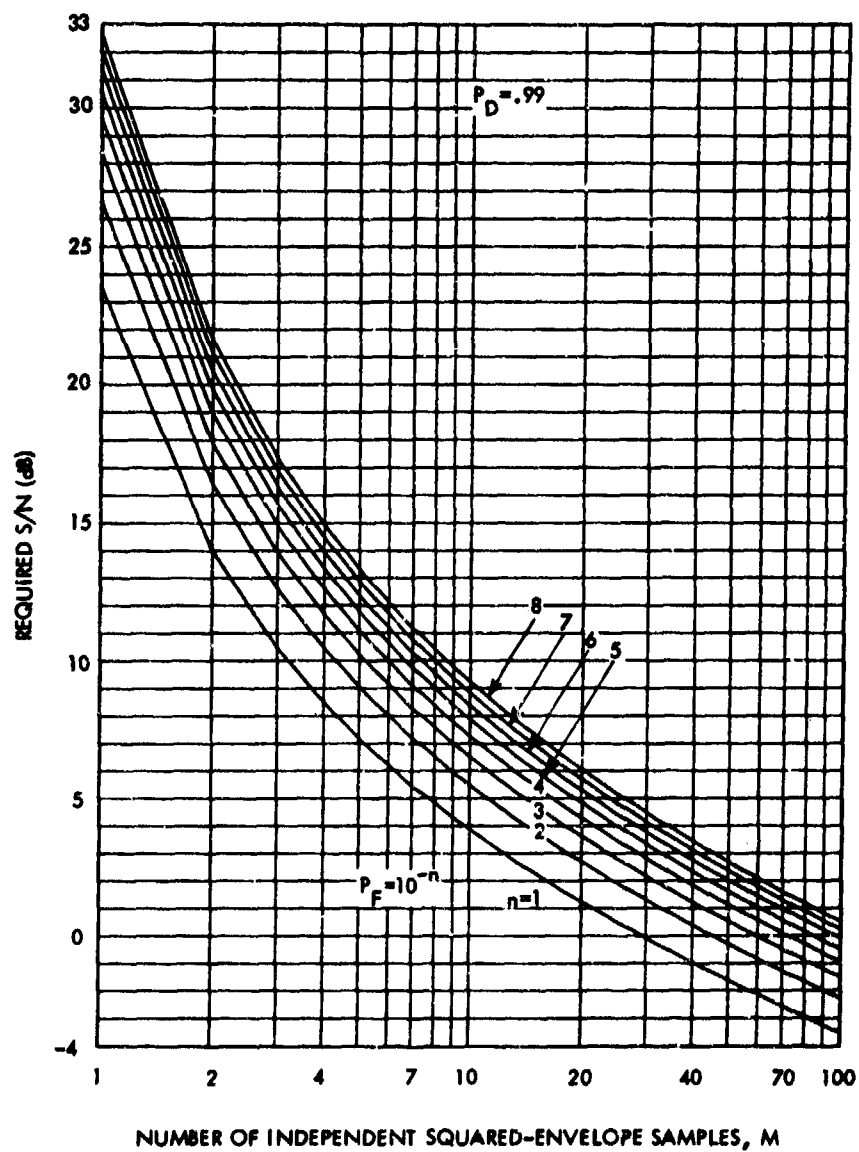


Figure 5. Required Signal-to-Noise Ratio for $P_D = .99$

It is anticipated that for large M the RV z in (3) could be approximated by a Gaussian RV. This is investigated in Appendix C, where the approximate S/N required for large M is given by (C-8) as

$$S/N \approx \frac{\Phi^{-1}(P_D) - \Phi^{-1}(P_F)}{\sqrt{M} - \Phi^{-1}(P_D)}, \quad (11)$$

where $\Phi^{-1}(\cdot)$ is the inverse $\Phi(\cdot)$ function (see (C-5)). Equation (11) is expected to be a good approximation only for $M \gg 1$, and only for P_D significantly less than $\Phi(\sqrt{M})$, a point that is discussed further in Appendix C.

A special case of (11) is provided by $P_D = .5$ (see (C-10)). Converted to decibels, (11) becomes

$$10 \log (S/N) \approx 10 \log (-\Phi^{-1}(P_F)) - 5 \log M; P_D = .5, \quad (12)$$

which has the familiar $5 \log M (\cong 5 \log (BT))$ decay associated with energy detection for large M . Equation (12) is plotted in figure 6 as dashed lines for $P_F = 10^{-1}$, 10^{-2} , 10^{-4} , and 10^{-8} , and the exact results are plotted as solid lines. The values of the additive constant in (12) are given in table 1 (see table 26.6 of reference 5).

Table 1. Additive Constant in (12)

P_F	$10 \log (-\Phi^{-1}(P_F))$
10^{-1}	1.08
10^{-2}	3.67
10^{-3}	4.90
10^{-4}	5.70
10^{-5}	6.30
10^{-6}	6.77
10^{-7}	7.16
10^{-8}	7.49

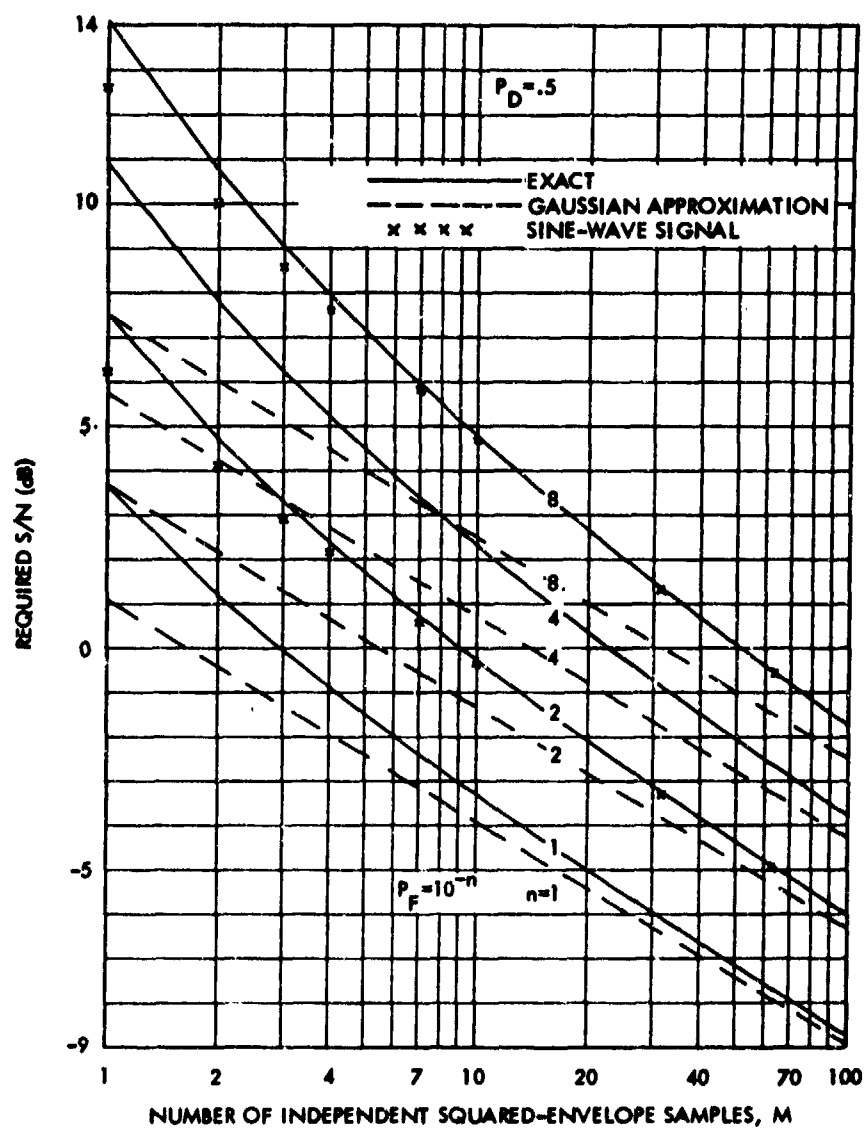


Figure 6. Comparison of Exact Results, Gaussian Approximation, and Sine-Wave Signal

Figure 6 shows that the exact results approach the Gaussian approximation asymptotically as M increases. However, even at $M = 100$, the Gaussian approximation is optimistic by 0.78 dB for $P_F = 10^{-8}$, 0.53 dB for $P_F = 10^{-4}$, and by only 0.19 dB for $P_F = 10^{-1}$.

For smaller M , such as $M = 10$, the Gaussian results are optimistic by 0.63, 1.07, 1.63, and 2.30 dB at $P_F = 10^{-1}$, 10^{-2} , 10^{-4} , and 10^{-8} , respectively, but for $M = 1$, they are optimistic by 2.58, 3.85, 5.20, and 6.59 dB, respectively. Thus the Gaussian approximation, and (12) in particular, should not be used unless M is very large compared with unity.

For other values of P_D , (11) can be converted into decibels and compared with the exact results. A sample calculation for $P_D = 0.9$, $P_F = 10^{-6}$, and $M = 10$ reveals that the exact S/N required is 3.29 dB, whereas the approximation (11) indicates 5.06 dB; thus the Gaussian approximation is optimistic by 1.23 dB in this case. It is worth noting, however, that this error is less than the corresponding error of 2.00 dB when $P_D = 0.5$, $P_F = 10^{-6}$, and $M = 10$. It is also worth noting that when $P_D = 0.9$, $P_F = 10^{-6}$, and $M = 100$, the exact S/N is -1.12 dB, whereas the approximation (11) indicates -1.60 dB; the discrepancy here is only 0.48 dB, which is again less than the 0.67 dB error for $P_D = 0.5$.

Generally, for $P_D \neq 0.5$, the approximation (11) does not plot as a straight line as in figure 6. Rather, the plot of (11) curves up sharply as M decreases and, in fact, goes to ∞ at $M = [\Phi^{-1}(P_D)]^2$. Thus approximation (11) can overestimate the required S/N for small enough M and $P_D > 0.5$. Also, as M increases from small values, (11) crosses the exact S/N curve and reaches a maximum undershoot before again approaching the exact S/N curve for large M . The net effect is that (11) is not a good approximation to use unless both $M \gg 1$ and $M \gg [\Phi^{-1}(P_D)]^2$.

If the signal were not a Gaussian process, but a sine wave, we could use the results of reference 6 (equations (B-21) through (B-25) and (C-13)) by identifying

$$\frac{d_T^2}{2} = M \ S/N \quad (13)$$

Equation (13) can be solved for S/N in terms of d_T . (Figures 2 through 14 in reference 6 provide the desired values of d_T .) We have plotted as X_s in figure 6 the required S/N , in decibels, for the sine-wave process for $P_F = 10^{-2}$ and 10^{-8} . Little difference is evident between the S/N required for a Gaussian signal process and that required for a sine-wave-signal process, except for very small values of M . The sine-wave-signal process requires a slightly lower value of S/N than does the Gaussian signal process — this conclusion is drawn only for the $P_D = 0.5$ case considered here.

CONCLUSIONS AND RECOMMENDATIONS

Rules of thumb for determining required SNR, such as those developed from a Gaussian approximation, are grossly optimistic predictions when the number of SE samples, $M(=BT + 1)$, is small. Because errors of many decibels can occur for M of the order of unity, the results shown in figures 2 through 5 should be preferred for performance predictions in narrowband energy detection. However, these results should still be considered as optimistic because, in practice, unavoidable center frequency and bandwidth mismatches of the analysis filter with respect to the signal spectrum occur and require larger values of SNR than are indicated in this report. (Bandwidth mismatch is considered quantitatively in reference 1.)

The false-alarm and detection probabilities themselves, not deflection criteria, are used as performance measures here. Also, no assumptions about the absolute or relative sizes of analysis bandwidth B and observation time T are required; only their product is important. The major approximation has been the replacement of BT by an effective number of independent SE samples, $M-1$. This approximation is difficult to be precise about, without an exact analysis as conducted in reference 7. (Details of the exact analysis for continuous detection are extremely tedious, as Appendix B in reference 7 attests.) It appears that the next order of business should be an exact analysis of the sampled system in figure 1 using the methods in references 8 and 9.

The results in this report are actually exact for a rectangular NBF, if BT is an integer; then, M is precisely $BT + 1$. This follows because every SE sample $\mathcal{E}^2(t_k)$ in figure 1 is statistically independent in the case of a rectangular NBF, and there are $T/B + 1$ samples in T (see Appendix A).

Appendix A

EQUIVALENT NUMBER OF INDEPENDENT SQUARED-ENVELOPE SAMPLES

The problem here is to find an equivalent number of independent, squared-envelope (SE) samples for the detector in figure 1 when the NBF and sampling increment are arbitrary and the SE samples are statistically dependent. With this information, the results of this report can be extended approximately to other signal spectra, filters, and sampling plans.

The observation interval available to the sampler in figure 1 is $(0, T)$, during which time an arbitrary number, N , of equi-spaced SE samples are taken. The time between SE samples is then $\Delta t = T/(N-1)$. A related problem that we will address is: What value of Δt should be chosen to make the best use of the available data?

The sum of N (dependent) SE samples in figure 1 is proportional to

$$u = \frac{1}{2N} \sum_{k=0}^{N-1} \varepsilon^2(k\Delta t) = \frac{1}{2N} \sum_{k=0}^{N-1} \varepsilon^2\left(\frac{kT}{N-1}\right) . \quad (\text{A-1})$$

Using the probability density function for the envelope given in (4), we see that the mean of RV u is

$$E\{u\} = \frac{1}{2} E\{\varepsilon^2(t)\} = \sigma^2 . \quad (\text{A-2})$$

Now

$$\varepsilon^2(t) = y_c^2(t) + y_s^2(t) , \quad (\text{A-3})$$

where $y_c(t)$ and $y_s(t)$ are the in-phase and quadrature components of the NBF output $y(t)$ (see reference 7, Appendix A). If, and only if, the spectrum $G_y(f)$ of Gaussian process $y(t)$ is symmetric about its center frequency f_0 , then $y_c(t)$ and $y_s(t)$ are independent Gaussian processes, each with correlation function

$$R_O(\tau) = \int_{-\infty}^{\infty} df \cos(2\pi f\tau) G_O(f), \quad R_O(0) = \sigma^2 , \quad (\text{A-4})$$

where

$$G_o(f) = \begin{cases} 2 G_y(f + f_o), & f > -f_o \\ 0, & f < -f_o \end{cases} \quad (A-5)$$

Then each SE sample is the sum of two independent samples.

The variance of u follows as

$$\text{Var}\{u\} = \frac{1}{N} \sum_{k=-N}^N \left(1 - \frac{|k|}{N}\right) R_o^2\left(\frac{kT}{N-1}\right) \quad (A-6)$$

Now let us consider a new RV v formed as the sum of M statistically independent SE samples:

$$v = \frac{1}{2M} \sum_{k=1}^M w_k^2 \quad (A-7)$$

RV v is a multiple of a chi-square variate with $2M$ degrees of freedom; it is also a scaled version of (3). We wish to approximate the statistics of the general RV u by those of RV v . In particular, we will set the means and variances of u and v equal. Using (4) and (A-4), we find

$$\begin{aligned} E\{v\} &= \sigma^2, \\ \text{Var}\{v\} &= \frac{1}{M} \sigma^4 = \frac{1}{M} R_o^2(0) \end{aligned} \quad (A-8)$$

The means of u and v are already equal and the variances can be made equal if we choose M in (A-7) (by equating (A-6) and (A-8)) according to

$$M = \frac{1}{\frac{1}{N} \sum_{k=-N}^N \left(1 - \frac{|k|}{N}\right) \frac{R_o^2\left(\frac{kT}{N-1}\right)}{R_o^2(0)}} \quad (A-9)$$

Equation (A-9) provides a definition of the equivalent number of independent SE samples in RV u . (Since the right-hand side of (A-9) is not necessarily an

integer, M could be chosen as the closest integer; then the variances of u and v would be approximately equal.) In the special case when Δt is chosen such that the samples of $\varepsilon^2(t)$ in (A-1) are all uncorrelated, then $R_0(k\Delta t) = 0$ for $k \neq 0$, and $M = N$.

Two special cases of (A-9) are worth noting. The first is that in the limit of continuous processing, $N \rightarrow \infty$, and (A-9) approaches

$$M_c = \frac{1}{\int_{-1}^1 dx (1 - |x|) \frac{R_o^2(Tx)}{R_o^2(0)}}. \quad (A-10)$$

The second is that if observation time T is large compared with the effective correlation time of $R_0(\tau)$, then (A-10) becomes,

$$M_c \cong \frac{1}{\int_{-\infty}^{\infty} dx \frac{R_o^2(Tx)}{R_o^2(0)}} = T \frac{\left[\int_{-\infty}^{\infty} df G_o(f) \right]^2}{\int_{-\infty}^{\infty} df G_o^2(f)} = T \frac{\left[\int_0^{\infty} dy G_y(f) \right]^2}{\int_0^{\infty} df G_y^2(f)} = BT, \quad (A-11)$$

where we have used (A-4), (A-5), and (2), and where B is the effective (or statistical) bandwidth of the positive-frequency component of the NBF in figure 1.

Returning to the general result for the equivalent number of independent SE samples, (A-9), we note from figures 2 through 5 that M is desired to be as large as possible. Therefore, we investigate the behavior of M in (A-9) as a function of N , and select that value of N corresponding to a maximum of M ; the best N will not be infinite (see reference 10).

We must investigate (A-9) through particular examples. The first example is a rectangular spectrum for the NBF output $y(t)$:

$$G_y(f) = \begin{cases} \frac{\sigma^2}{2B}, & |f \pm f_0| < \frac{1}{2} B \\ 0, & \text{otherwise} \end{cases},$$

$$G_o(f) = \begin{cases} \frac{\sigma^2}{B}, & |f| < \frac{1}{2} B \\ 0, & \text{otherwise} \end{cases}, \quad (\text{A-12})$$

$$R_o(\tau) = \sigma^2 \frac{\sin(\pi B \tau)}{\pi B \tau} \equiv \sigma^2 \text{sinc}(B \tau).$$

Substitution of (A-12) in (A-9) yields

$$M = \frac{1}{\frac{1}{N} \sum_{k=-N}^N \left(1 - \frac{|k|}{N}\right) \text{sinc}^2\left(\frac{kBT}{N-1}\right)}. \quad (\text{A-13})$$

The quantity M is a function only of the BT product and the particular value of N selected and is plotted versus N for several BT products in figure A-1. It will be observed that M increases nearly linearly with N until M saturates at approximately the value $BT+1$ when $N = BT+1$. The corresponding Δt is $T(N-1) = 1/B$; that is, the SE samples are uncorrelated* ($R_o(k\Delta t) = 0$ for $k \neq 0$) when taken at the bandwidth rate of the NBF. (Although M can be made slightly larger than $BT+1$ by choosing N one larger than $BT+1$, i. e., $\Delta t < 1/B$, the gain is negligible.) Thus for the rectangular spectrum, we have $\Delta t = 1/B$, $M = BT+1$.

The second example is a Gaussian spectrum,

$$G_o(f) = \frac{\sqrt{2}\sigma^2}{B} \exp(-2\pi f^2/B^2), \quad (\text{A-14})$$

$$R_o(\tau) = \sigma^2 \exp\left(-\frac{\pi}{2} B^2 \tau^2\right).$$

The plot of M versus N is given in figure A-2. As in the case of a rectangular spectrum, M saturates at approximately the value $BT+1$ when N equals $BT+1$, and $\Delta t = 1/B$ is again the recommended sampling interval. However, the SE samples are no longer statistically independent; instead, adjacent SE samples have a correlation coefficient* of $\exp(-\pi) = 0.043$.

*The correlation coefficient of $\varepsilon^2(t)$ is $R_o^2(\tau)/R_o^2(0)$.

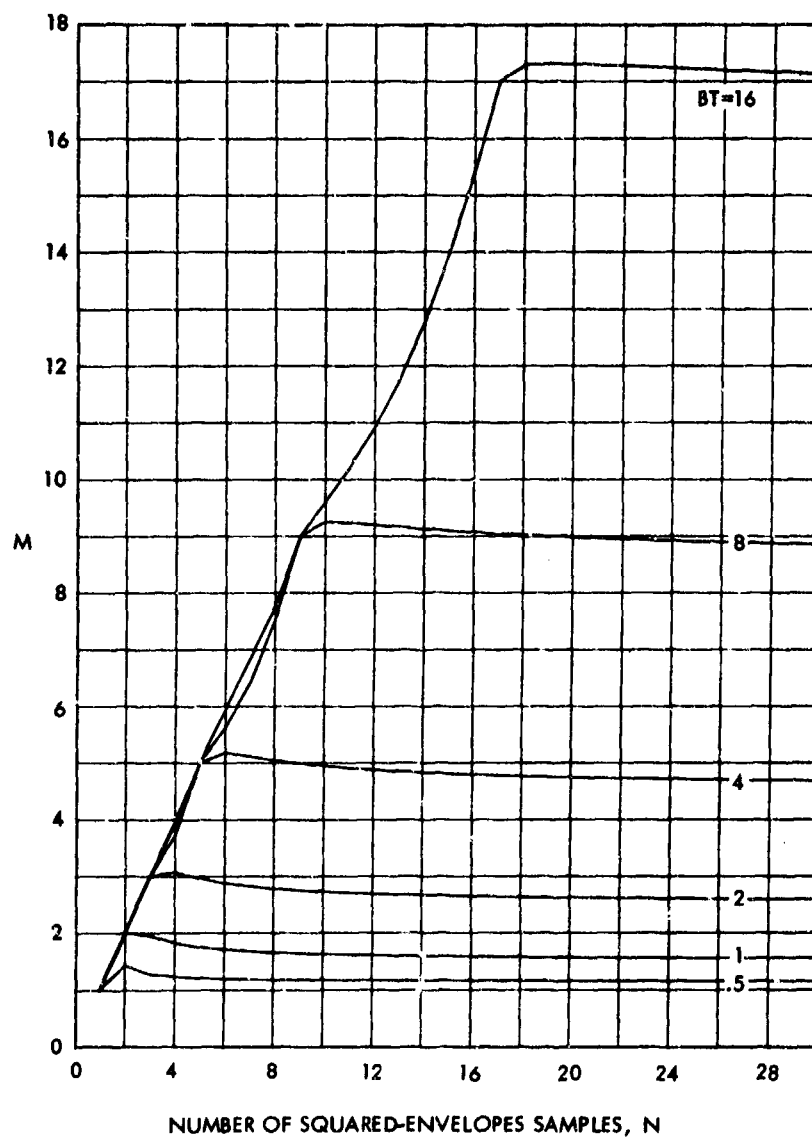


Figure A-1. Equivalent Number of Independent Squared-Envelope Samples for Rectangular Spectrum

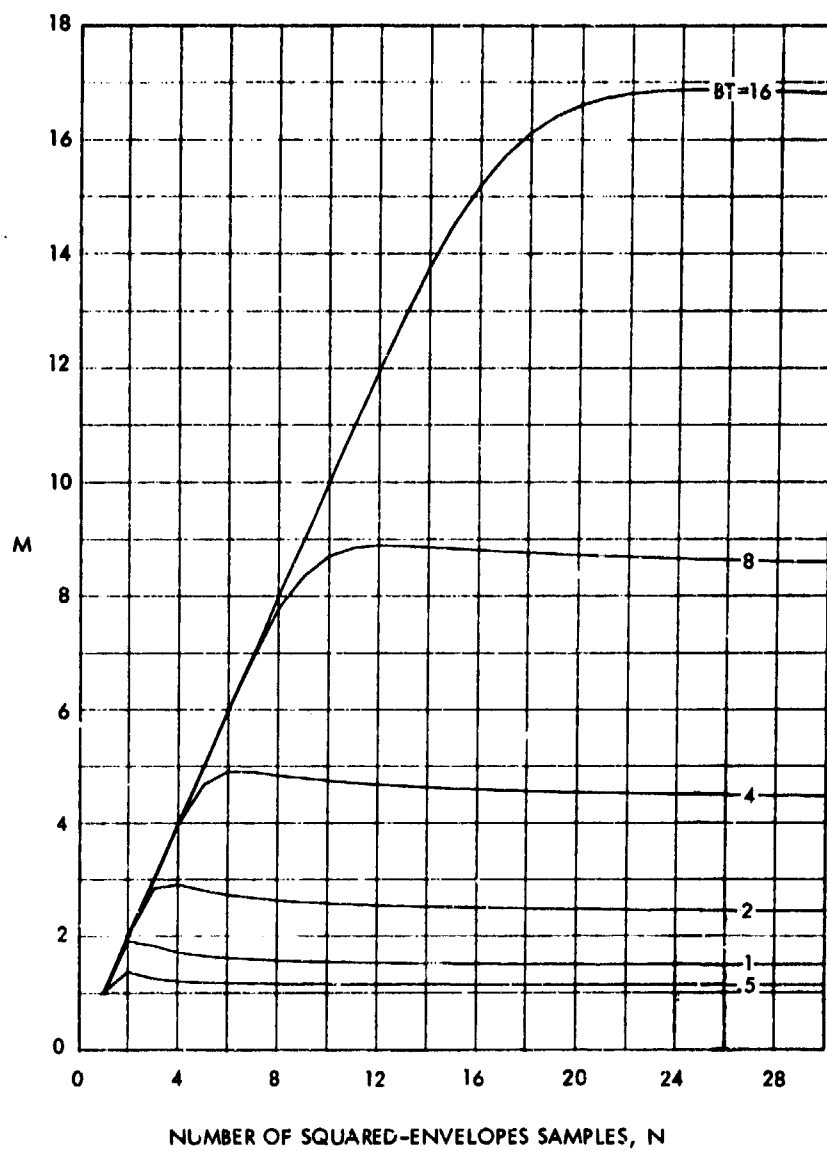


Figure A-2. Equivalent Number of Independent Squared-Envelope Samples for Gaussian Spectrum

The third example is a Cauchy spectrum,

$$G_o(f) = 2\sigma^2 \frac{B}{(2\pi f)^2 + B^2} ,$$

$$R_o(\tau) = \sigma^2 \exp(-B|\tau|) .$$
(A-15)

The plot of M versus N is given in figure A-3. Although M again saturates for large N approximately at the value $BT + 1$, the value of N required is larger than $BT + 1$. In fact, a value of N approximately equal to $2BT$ is required to realize the saturation value of M . In this case, the sampling increment Δt equals $1/(2B)$ and the SE samples are highly correlated, the correlation coefficient of adjacent SE samples being $1/e = 0.37$.

Thus, for three widely different spectra, the equivalent number of independent SE samples is given approximately by $BT + 1$, where B is the effective bandwidth of the NBF output spectrum. The sampling increment should be approximately $1/B$ for fairly-rectangular passband characteristics, but must be smaller than this amount for rounded filter characteristics.

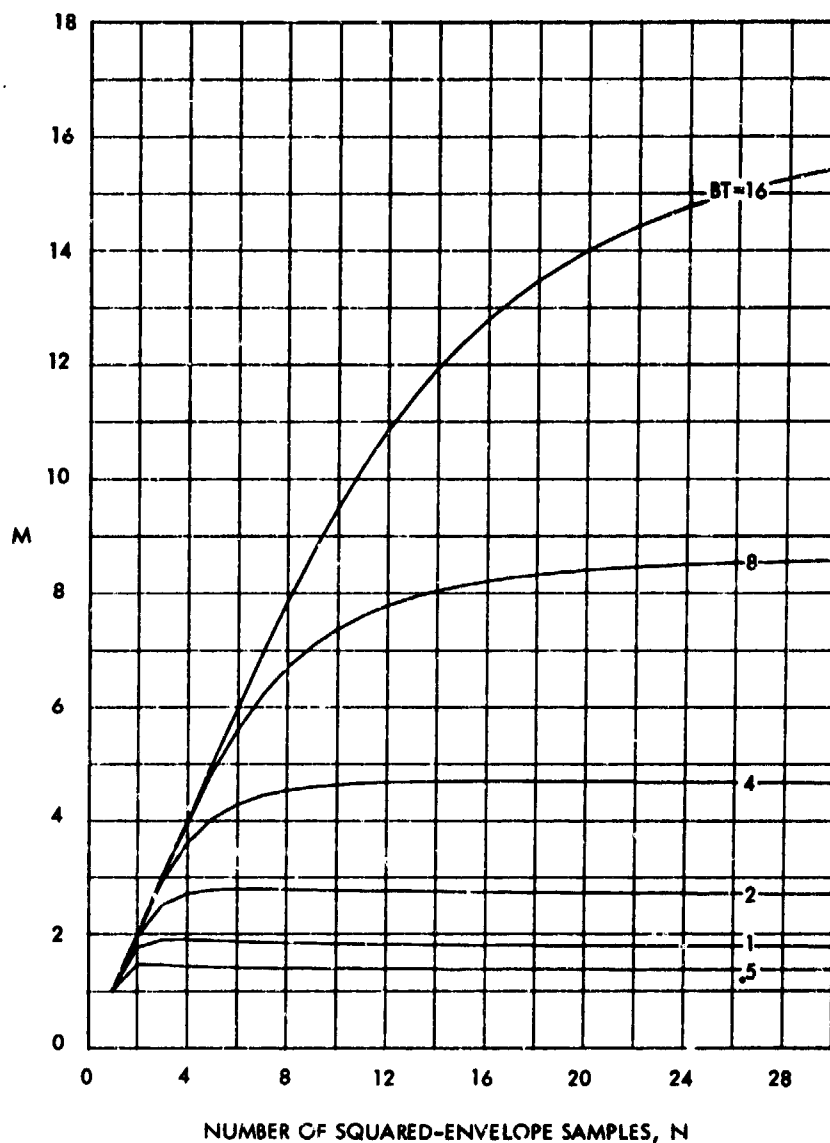


Figure A-3. Equivalent Number of Independent Squared-Envelope Samples for Cauchy Spectrum

Appendix B THRESHOLD VALUES

The false alarm probability is given in (7). Values of the normalized threshold $A = \Lambda / (2N)$ required to realize specified values of P_F are given in table B-1.

Table B-1. Normalized Threshold Values A

M	P_F							
	10^{-1}	10^{-2}	10^{-3}	10^{-4}	10^{-5}	10^{-6}	10^{-7}	10^{-8}
1	2.303	4.605	6.908	9.210	11.512	13.816	16.118	18.421
2	3.890	6.638	9.233	11.756	14.237	16.688	19.120	21.536
3	5.322	8.406	11.229	13.928	16.554	19.129	21.669	24.181
4	6.681	10.045	13.062	15.914	18.666	21.350	23.986	26.585
5	7.994	11.605	14.794	17.782	20.648	23.431	26.155	28.832
6	9.275	13.108	16.455	19.567	22.538	25.413	28.217	30.967
7	10.532	14.571	18.062	21.290	24.358	27.318	30.198	33.016
8	11.771	16.000	19.626	22.962	26.122	29.162	32.114	34.997
9	12.995	17.403	21.156	24.595	27.841	30.957	33.977	36.922
10	14.206	18.783	22.657	26.193	29.522	32.710	35.795	38.799
16	21.292	26.743	31.244	35.286	30.047	42.616	46.042	49.359
32	39.430	46.608	52.358	57.417	62.052	66.394	70.519	74.477
64	74.443	84.067	91.593	98.106	103.995	109.453	114.592	119.482

If the mean value of decision variable z in figure 1 is subtracted before threshold comparison, the number of standard deviations that the new threshold must be set at is given (for signal absent) by

$$\frac{\Lambda - E\{z\}}{\text{St. Dev. } \{z\}} = \frac{\Lambda - M \cdot 2N}{\sqrt{M} \cdot 2N} = \frac{\Lambda}{\sqrt{M}} - \sqrt{M} \quad (\text{B-1})$$

The results in table B-1 may be substituted in equation (B-1) to find the new thresholds. For example, $M = 64$, $P_F = 10^{-3}$ requires a threshold set at 3.449 standard deviations.

Appendix C

GAUSSIAN APPROXIMATION

For large M , RV z in (3) tends toward a Gaussian RV. It follows from (5) that

$$E\{z^k\} = \frac{(M-1+k)!}{(M-1)!} (2\sigma^2)^k \quad (C-1)$$

In particular,

$$\begin{aligned} E\{z\} &= M 2\sigma^2, \\ \text{Var}\{z\} &= M(2\sigma^2)^2. \end{aligned} \quad (C-2)$$

Then,

$$p(z) \approx \frac{1}{\sqrt{2\pi M} 2\sigma^2} \exp\left[-\frac{(z - M 2\sigma^2)^2}{2M(2\sigma^2)^2}\right], \quad (C-3)$$

and

$$\text{Prob}(z > \Lambda) \approx \Phi\left(\sqrt{M} - \frac{1}{\sqrt{M}} \frac{\Lambda}{2\sigma^2}\right), \quad (C-4)$$

where

$$\Phi(x) = \int_{-\infty}^x dt (2\pi)^{-1/2} \exp(-t^2/2). \quad (C-5)$$

An immediate problem of the Gaussian approximation is indicated by (C-4): as $\sigma^2 \rightarrow \infty$, the right-hand side of (C-4) tends to $\Phi(\sqrt{M})$, which is less than 1. Thus arbitrarily high detection probabilities can never be realized by the Gaussian approximation unless $M \gg 1$. This is not true of the exact distribution of z for any M , as (6) shows that the $\text{Prob}(z > \Lambda) \rightarrow 1$ as $\sigma^2 \rightarrow \infty$.

The approximations to P_F and P_D are obtained by using (1) and (9) in (C-4):

$$P_F \approx \Phi\left(\sqrt{M} - \frac{1}{\sqrt{M}} A\right) \quad (C-6)$$

$$P_D \approx \Phi\left(\sqrt{M} - \frac{1}{\sqrt{M}} \frac{A}{1 + S/N}\right) \quad (C-7)$$

Equations (C-6) and (C-7) may be solved for S/N (by eliminating A) to obtain

$$S/N \approx \frac{\Phi^{-1}(P_D) - \Phi^{-1}(P_F)}{\sqrt{M} - \Phi^{-1}(P_D)} \quad (C-8)$$

where $\Phi^{-1}(\)$ is the inverse $\Phi(\)$ function. (The impossibility of requiring $P_D > \Phi(\sqrt{M})$ is now made obvious by the denominator of (C-8).)

For large M , (C-8) decays as $M^{-1/2}$, regardless of the choice of P_D and P_F . However, the point at which this behavior develops depends upon how large P_D is.

A special case of (C-8) is provided by $P_D = .5$; then $\Phi^{-1}(P_D) = 0$ and

$$S/N \approx \frac{-\Phi^{-1}(P_F)}{\sqrt{M}}; P_D = .5 \quad (C-9)$$

Converted to decibels, (C-9) is

$$10 \log (S/N) \approx 10 \log \left(-\Phi^{-1}(P_F) \right) - 5 \log M; P_D = .5 \quad (C-10)$$

LIST OF REFERENCES

1. D. W. Hyde and A. H. Nuttall, "Square-Law Detection of Narrow-Band Processes," NUSC Technical Memorandum 2020-5-70, 14 January 1970.
2. A. H. Nuttall and P. G. Cable, Operating Characteristics for Maximum Likelihood Detection of Signals in Gaussian Noise of Unknown Level; I. Coherent Signals of Unknown Level, NUSC Technical Report 4243, 27 March 1972.
3. S. O. Rice, "Mathematical Analysis of Random Noise," Bell System Technical Journal, vol. 23, pp. 283-332, 1944, and vol. 24, pp. 46-156, 1945.
4. C. W. Helstrom, Statistical Theory of Signal Detection, Pergamon Press, N. Y., 1960.
5. Handbook of Mathematical Functions, U. S. Department of Commerce, National Bureau of Standards, Applied Math Series, No. 55, June 1964.
6. A. H. Nuttall and R. Garber, "Receiver Operating Characteristics for Phase-Incoherent Detection of Multiple Observations," NUSC Technical Memorandum TC-179-71, 28 September 1971.
7. A. H. Nuttall and D. W. Hyde, Operating Characteristics for Continuous Square-Law Detection in Gaussian Noise, NUSC Technical Report 4233, 3 April 1972.
8. A. H. Nuttall, Numerical Evaluation of Cumulative Probability Distribution Functions Directly from Characteristic Functions, NUSC Technical Report 1032, 11 August 1969. Also Proceedings of the IEEE, vol. 57, no. 11, November 1969, pp. 2071-2072.
9. A. H. Nuttall, Alternate Forms and Computational Considerations for Numerical Evaluation of Cumulative Probability Distributions Directly from Characteristic Functions, NUSC Technical Report 3012, 12 August 1970. Also Proceedings of the IEEE, vol. 58, no. 11, November 1970, pp. 1872-1873.
10. A. H. Nuttall, "Relative Performance of Integrator and Equi-Weighted Sampler in Estimation of Mean of Random Process," NUSC Technical Memorandum TC-87-72, 24 April 1972.